

Enhanced Pinning of Vortices in Thin Film Superconductors by Magnetic Dot Arrays

R. Šášik* and T. Hwa†

*Institute for Pure and Applied Physics, University of California at San Diego, 9500 Gilman Drive, La Jolla, CA 92093-0360

†Department of Physics, University of California at San Diego, 9500 Gilman Drive, La Jolla, CA 92093-0319

(October 28, 2018)

We study the pinning of vortices in thin film superconductors by magnetic dots in the London approximation. A single dot is in general able to pin *multiple* field-induced vortices, up to a saturation number n_s , which can be much larger than one. However, the magnetic field of the dot also creates *intrinsic* vortices and anti-vortices, which must be accounted for. In a ferromagnetic dot array, the intrinsic anti-vortices are pinned only interstitially. Much stronger pinning effect is expected of an antiferromagnetic dot array. Possible realizations of various magnetic configurations are discussed.

PACS numbers: 74.60.Ge, 74.80.Dm, 75.50.Tt

Artificially patterned sub-micron magnetic structures hold a great promise not only for magnetic device and storage technology, but also as a tool of fundamental research when used as a means of controlling other physical systems, such as the two-dimensional electron gas [1] and vortices in superconductors [2–4]. It is an experimental fact that when a type-II superconducting film is deposited over a regular array of magnetic dots, resistivity of the film exhibits a series of sharp minima as a function of the applied magnetic field, with the positions of the minima being integer multiples of the geometrical “matching field” of the magnetic lattice [2]. In contrast, no periodic pinning was found in a similar system with a regular array of *non-magnetic* defects [2]. This suggests the importance of the magnetization of the dots in producing low resistivity, although the exact flux pinning mechanism has not been fully understood. A recent study by Lyuksyutov and Pokrovsky [5] explored various statistical mechanics issues that might arise from the complexity of the magnet-superconductor interaction. In this work, we focus on the pinning mechanism itself, the understanding of which will lead us to desirable magnetic dot structures that enhance vortex pinning for a range of applied magnetic fields.

We study the low temperature properties of a superconducting thin film such as Nb deposited on top of a regular array of magnetic dots, separated by a thin insulating layer to suppress the proximity effect (Fig. 1). The superconductor has a magnetic penetration length λ much larger than the coherence length ξ , and the film is taken to be a homogeneous thin plate of thickness $d \ll \lambda$. For the magnetic dots, we assume the magnetization on each dot to be *quenched in*, and pointing normal to the layer. In what follows, we will investigate how the interaction between vortices in the superconductor is affected by the magnetic dots, and explore which quenched configurations of magnetization are favorable for vortex pinning at low temperatures. At the end, we will discuss how the desired configuration(s) of magnetization might be achieved in practice.

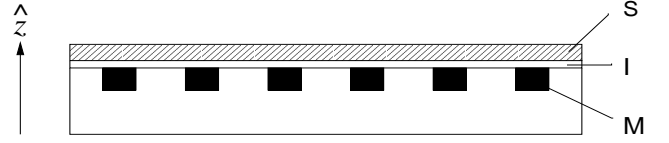


FIG. 1. Schematic diagram of the superconducting layer (S) deposited over an array of magnetic dots (M), separated with a thin insulating layer (I).

We first describe the case of a *single* dot with magnetization $\mathbf{M}(\mathbf{r})$ to be specified shortly. Modeling the thin-film superconductor as an ideal sheet current $\mathbf{K}_s(\vec{\rho})$ at the $z = 0$ plane (with $\vec{\rho} \equiv [x, y]$ denoting the position vector), Maxwell’s equation of magnetostatics becomes

$$-\nabla^2 \mathbf{A}(\mathbf{r}) = \frac{4\pi}{c} \mathbf{K}_s(\vec{\rho}) \delta(z) + 4\pi \nabla \times \mathbf{M}(\mathbf{r}), \quad (1)$$

in the gauge $\nabla \cdot \mathbf{A} = 0$. We will describe the superconductor in the London approximation [6], which has $\mathbf{K}_s(\vec{\rho}) = (c/4\pi\lambda) \cdot [\vec{\Phi}(\vec{\rho}) - \mathbf{A}(\vec{\rho})]$, where $\Lambda \equiv \lambda^2/d$ is the relevant magnetic length scale for the superconducting film, and $\vec{\Phi}(\vec{\rho})$ is the London vector which, for a collection of vortices located at points $\vec{\rho}_j$ with respective quantization (charges) ϵ_j , is

$$\vec{\Phi}(\vec{\rho}) = \frac{\phi_0}{2\pi} \sum_j \epsilon_j \frac{\hat{z} \times (\vec{\rho} - \vec{\rho}_j)}{(\vec{\rho} - \vec{\rho}_j)^2}. \quad (2)$$

The above form of \mathbf{K}_s holds everywhere except at the vortex cores, which are normal regions of radius $\sim \xi$ around each singularity, and for as long as $\hat{z} \cdot \mathbf{A}(\vec{\rho}) = 0$, which will be satisfied in our case. Using the superposition principle, we write $\mathbf{A}(\mathbf{r}) = \mathbf{A}_s(\mathbf{r}) + \mathbf{A}_m(\mathbf{r})$, where \mathbf{A}_s is the magnetic vector potential due to the supercurrent, and \mathbf{A}_m is the vector potential due to the magnetic dot. In what follows, we will model a magnetic dot by a *perfect dipole* of magnetic moment $\mathbf{m} \equiv m\hat{z}$, placed at a distance ℓ below the superconducting plane and the origin. Thus,

$\mathbf{A}_m(\mathbf{r}) = m(\hat{z} \times \mathbf{r})/|\mathbf{r} + \ell\hat{z}|^3$. The dipole model is exact, of course, only for homogeneous spherical magnetic dots. Nevertheless, we will use this dipolar approximation throughout, in the hope that the results will give the correct order of magnitude for a variety of magnets whose magnetizations are normal to the plane.

The free energy of the entire system may be written as

$$F = \frac{1}{2c} \int d^2\vec{\rho} \left[\frac{4\pi\Lambda}{c} |\mathbf{K}_s(\vec{\rho})|^2 + \mathbf{A}_s(\vec{\rho}) \cdot \mathbf{K}_s(\vec{\rho}) \right] - \mathbf{m} \cdot \nabla \times \mathbf{A}_s|_{\mathbf{r}=-\ell\hat{z}}. \quad (3)$$

The term in [...] is the sum of the kinetic and magnetic field energies of the supercurrent; the last term is the potential energy of the magnetic dipole in the magnetic field of the supercurrent. Using Eq. (1), we can integrate out the vector potential and express the free energy completely in terms of the vortices in the superconductors. We have $F = F_{vv} + F_{vm}$, where

$$F_{vv} = \frac{\phi_0^2}{16\pi^2\Lambda} \sum_{i,j} \epsilon_i \epsilon_j U(|\vec{\rho}_j - \vec{\rho}_i|), \quad (4)$$

is the vortex-vortex interaction energy (including the vortex self-energy), with $U(\rho)$ being the Pearl potential [7] whose asymptotic behavior is

$$U(\rho) \sim \begin{cases} \ln(\Lambda/\xi), & \rho \ll \xi, \\ (1/2) \ln(\Lambda/\rho), & \xi \ll \rho \ll \Lambda, \\ \Lambda/(2\rho), & \rho \gg \Lambda, \end{cases} \quad (5)$$

and

$$F_{vm} = \frac{\phi_0 m}{\pi\Lambda^2} \sum_j \epsilon_j V(|\vec{\rho}_j|), \quad (6)$$

is the vortex-magnet interaction, with

$$V(\rho) \equiv - \int_0^\infty d\kappa \frac{\kappa e^{-\kappa\ell/\Lambda}}{2\kappa + 1} J_0(\kappa\rho/\Lambda) \sim \begin{cases} -\Lambda/2\ell, & \rho \ll \ell \ll \Lambda, \\ -\Lambda/2\rho, & \ell \ll \rho \ll \Lambda, \\ -2(\Lambda/\rho)^3, & \rho \gg \Lambda. \end{cases} \quad (7)$$

We will assume that $\rho \ll \Lambda$ and $\ell \sim \xi$, which correspond to the more interesting and experimentally realistic cases. A single magnetic dipole with $m > 0$ is in general able to bind more than one vortex. The attractive force on a vortex due to the magnet is the strongest at a distance $\sim \ell$ from the magnet. Since the vortex-vortex repulsion decays only logarithmically with distance, we conclude that all bound vortices are concentrated in an area of radius $\sim \ell$ around the dot. When their number is large (and it can be), they can be considered a single multiply quantized vortex, since $\ell \sim \xi$ by assumption.

The maximum charge n_s of the bound vortex can be found as follows: Suppose the net vorticity of the sample

(as enforced by the application of an external magnetic field) is $N > n_s$, and out of these N vortices, there is a vortex of charge n at the origin above the dot, with the remaining $N - n$ vortices singly quantized and far removed from each other and from the origin. The total free energy of such a system is simply

$$F(n) = \frac{\phi_0^2}{16\pi^2\Lambda} (n^2 + N - n) \ln \frac{\Lambda}{\xi} + \frac{\phi_0 m}{\pi\Lambda^2} n V(0). \quad (8)$$

n_s can then be identified as the value of n which minimizes $F(n)$, with the result

$$n_s = \text{int} \left[\frac{1}{2} + \frac{4\pi m}{\phi_0 \ell \ln(\Lambda/\xi)} \right], \quad (9)$$

where $\text{int}[x]$ denotes the nearest integer to x . The numerical value of n_s , which we shall call hereafter the *saturation number*, may be much larger than 1. As an example, let us consider a “typical” magnetic dot made of Co/Pt multilayer, with magnetization $\sim 500 \text{ emu cm}^{-3}$ [8], dot size $(0.25\mu\text{m})^2$ and height $h \sim 40 \text{ nm}$. Taking ℓ to be $h/2$, we get $m/\ell \sim 3\phi_0$. The factor $\ln(\Lambda/\xi)$ is given by the superconducting film itself; for Nb thin films somewhat below T_c with $\xi \sim 20 \text{ nm}$, $\lambda/\xi \sim 15$ and thickness $d \sim \xi$ one has $\ln(\Lambda/\xi) \sim 5$. In this case $n_s \approx 8$. This example illustrates that magnetic pinning may be many times more effective than pinning by material defects (e.g., holes) at the same density, since the holes can directly bind only one vortex per site. The ability of a single magnet to bind so many vortices is perhaps the most desirable property of the magnetic dot system, at least for the purpose of vortex pinning; this property has however not been recognized previously [5].

Extrapolating the above-described properties of a single dot to systems with many dots, one might naively conclude that an array of dots in the ferromagnetic configuration would provide the strongest pinning. Indeed, if the applied magnetic field is n_s times the matching field B_ϕ , then each dot will bind n_s field-induced vortices, a task not achievable by an array of non-magnetic pins if n_s is large. However, the ferromagnetic dot array suffers from a different problem: It has difficulty pinning at small applied fields, i.e., for $B \ll n_s B_\phi$, because of the appearance of *intrinsic* vortices and anti-vortices created by the magnetic field of the magnets themselves.

To understand the effect associated with intrinsic vortices, let us again consider the single-dot system, but now in the absence of any external magnetic field. For weak magnets, no vortex is created in the superconducting film. Vortices eventually appear in the film for sufficiently strong magnets. This first happens when there is a *doubly* quantized vortex bound directly above the magnet, with two single anti-vortices straddling it, each at a distance ρ_0 away [9]. The anti-vortices must be present in a large film (of linear size $\gg \ell$), since the net magnetic flux through the x - y plane due to the magnet is zero. (This important

fact was left out of the model in Ref. [5].) Annihilation of the anti-vortices with the nucleus is prevented by the short-range repulsion between the anti-vortices and the magnet. To find the onset of intrinsic vortices, we compute the free energy $F(\rho)$ obtained by applying the forms of the vortex-vortex and vortex-magnet interactions [Eqs. (4) and (6)] to the vortex-antivortex configuration described above. We take ρ_0 to be the value of ρ which minimizes $F(\rho)$, with the result $\rho_0 = 16\pi m/(3\phi_0)$. Intrinsic vortices appear when $F(\rho_0) < 0$, since the free energy of the system without vortices is set at $F = 0$ by definition. In the experimentally relevant limit $\rho_0 \gg \xi$, this occurs when the magnetization reaches a critical value $m_c = \frac{3}{8\pi}\phi_0\ell\ln(\Lambda/\xi)$. Using this expression for m_c , we can rewrite Eq. (9) as $n_s = \text{int}[\frac{1}{2} + \frac{3m}{2m_c}]$. Note that $n_s = 2$ when $m = m_c$. Thus, intrinsic vortices and anti-vortices will appear once the magnet becomes a better pinning site than a simple void, i.e., for $n_s > 1$.

Next, let us consider the behavior of a *ferromagnetic* (FM) square array of dots with $m > m_c$ and lattice constant $a \sim \rho_0$, again in the absence of any external magnetic field. In the Co/Pt example mentioned above, $a \sim \rho_0 \sim 1\mu\text{m}$. In this case, the intrinsic anti-vortices are very loosely associated with the magnetic dots and form a classical plasma, which interacts with the FM array only interstitially. For $n_s \gg 1$, the interstitial pinning is of high order and therefore very weak. Consequently, the anti-vortices can be set into motion by a small applied current or thermal excitation, leading to dissipation even in the absence of any applied field! This is certainly not a desirable feature for the purpose of vortex pinning.

The pinning ability of the FM array increases for increasing external fields, whose effect is mainly to annihilate a fraction of the intrinsic anti-vortices at interstitial sites. The annihilation is complete when the applied field reaches the order of $n_s B_\phi$ as already described above. Thus maximum critical current is obtained at this field. Through this consideration, we see that the main effect produced by the ferromagnetic array is to *shift* the zero of the magnetic field to some large value, i.e., $n_s B_\phi$. This can be utilized in special applications which requires a high critical current for a *given* field, but is not good in general, where high critical current is demanded for a *range* of external fields.

The pinning properties of the sample in low applied fields can be significantly improved if the magnets form a quenched square *antiferromagnetic* (AFM) array, where the intrinsic anti-vortices produced by those magnets in the $+\hat{z}$ (or “up”) direction tend to be attracted to the magnets in the $-\hat{z}$ (or “down”) direction. For strong magnets whose binding distance ρ_0 (between the magnet and its satellite anti-vortices) is of the order a , the anti-vortices will be pinned strongly to magnets pointed in the opposite direction, leading to a much larger critical current needed to dislodge the intrinsic vortices and anti-vortices at low fields.

In the absence of any external field, the free energy per unit cell of an AFM square array is obtained from Eqs. (4) and (6), assuming that n intrinsic vortices are localized on each upward magnets and n intrinsic anti-vortices are localized on each downward magnet. To sum the resulting alternating series of potential energies, a good approximation is to take the two largest terms of the series, which has a minimum when $n = n_s$.

In the presence of an external magnetic field, the field-induced vortices are subject to a periodic potential landscape created by the magnets and the bound intrinsic vortices and anti-vortices. To characterize this potential, we place a “test” vortex of charge $+1$ at some position $\vec{\rho}$, and compute the free energy $W(\vec{\rho})$ experienced by this test vortex, due to interaction with all the intrinsic vortices and anti-vortices, $n_{i,j} = (-1)^{i+j}n_s$, and with all the magnets, $m_{i,j} = (-1)^{i+j}m$, on the respective lattice sites $\vec{R}_{i,j} = a(i\hat{x} + j\hat{y})$. The resulting expression

$$W(\vec{\rho}) = \frac{\phi_0^2}{8\pi^2\Lambda} \sum_{i,j} n_{i,j} U(|\vec{\rho} - \vec{R}_{i,j}|) + \frac{\phi_0}{\pi\Lambda^2} \sum_{i,j} m_{i,j} V(|\vec{\rho} - \vec{R}_{i,j}|), \quad (10)$$

is plotted in Fig. 2 for the example in the text with $n_s = 8$ and $a = \rho_0/2$.

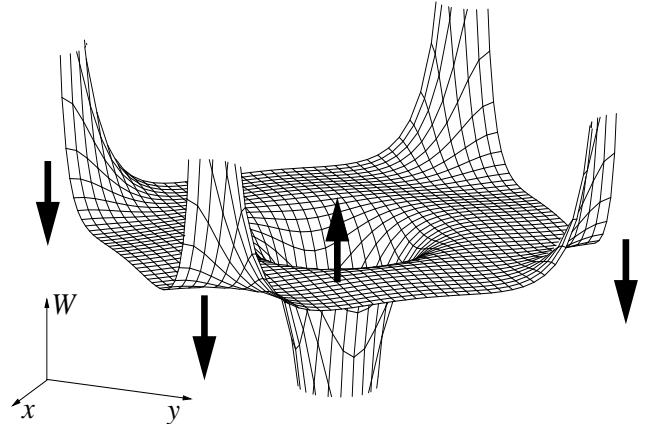


FIG. 2. Free energy $W(\vec{\rho})$ of a test vortex in an AFM dot array. The range of $W(\vec{\rho})$ is $\pm\phi_0^2 n_s/(16\pi^2\Lambda)$; $\vec{\rho}$ spans the primitive cell of the AFM lattice. The arrows indicate magnetic moments of the dots on the lattice sites.

The form of $W(\vec{\rho})$ clearly indicates that the test vortex will be attracted towards the nearest “up” magnet. Note that even though a magnet is already saturated with intrinsic vortices, it can still bind more field-induced vortices because there is no core energy cost associated with the latter. The maximum number of field-induced vortices n_c that an upward magnet can bind is estimated as follows: Every field-induced vortex (per primitive cell) that is attracted to the upward magnet changes the potential landscape for the test vortex. These bound

vortices surround the nucleus, effectively increasing its charge. A test vortex will no longer tend to the magnet when the repulsion from the effective charge of the nucleus becomes equal to the maximum attractive force due to the magnet. The latter force is strongest at a finite distance D ; in the point dipole approximation, Eq. (6), $D \sim \ell$. More realistically, D will be of order of the radius of the magnetic dot. The balance of forces gives

$$n_c \approx n_s \left(\frac{2\ell}{D} \ln \frac{\Lambda}{\xi} - 1 \right). \quad (11)$$

In our example system, where $D \sim 0.1 \mu\text{m}$, $n_c \sim n_s$.

The analysis described in this study suggest very different behaviors for a superconducting thin film on a (quenched) FM or AFM dot array. For the FM array, we expect the system to have low critical current J_c at low fields, with successively increasing J_c when the applied field is an integer multiple of the matching field, and with the maximal J_c obtained at $B = n_s B_\phi$. For the AFM array, we expect the pinning to be the strongest at low fields, with successively lower J_c as the applied field reaches higher and higher orders of the matching field, and with the main effect diminishing beyond a field value of $n_c B_\phi/2$. Thus, for different applications, one might want to use one or the other type of arrays, or some combination.

It remains to address how the quenched magnetic dot configurations can be achieved and maintained in an applied field. The FM array is most easily prepared by aligning the magnetic moments in a strong magnetic field in the z direction prior to measurement. It is less straightforward to ensure the AFM arrangement. Fortunately, we are aided in this case by the fact that the AFM state is the *ground state* of a square lattice of magnetic dipoles as long as the out-of-plane direction (i.e., the \hat{z} axis) is the “easy” magnetization axis [10]. The latter can be arranged by the construction of the individual magnetic dot, e.g., by using the multi-layer Co/Pt structure [11]. The appearance of intrinsic vortices further stabilizes the AFM structure. Thus, the AFM array will in fact form *spontaneously* upon cooling from high temperature in zero applied field, based on purely energetic considerations. There are, of course, kinetic constraints, such as coercive effects and the mobility of the domain wall separating the two degenerate states of the antiferromagnet, that may prevent a perfect antiferromagnet from being formed at a reasonable time. These kinetic constraints are, on the other hand, necessary to prevent the magnets to undergo a spin-flop type transition [12] to the FM phase upon increasing the external magnetic field. One can also envision building an array of microscopic superconducting current rings below the film, and electronically control the sense of current in each ring. This way, arbitrary quenched magnet configurations can be specified.

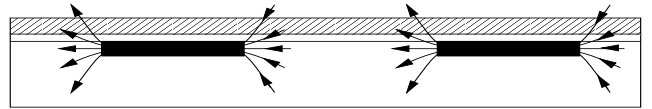


FIG. 3. Schematic diagram of the superconducting layer with thin magnetic rods magnetized horizontally.

A practical way to achieve effects similar to that of the AFM array is to bury under the superconductor an array of thin magnetic *bars* (Fig. 3). The shape anisotropy of the bar will force the magnetization to be along the length of the magnet. The field outside the magnet is the same as that of two oppositely charged magnetic monopoles located at its endpoints, creating an effect similar to that of an antiferromagnetic pair of dipoles whose moments are normal to the sample [13]. A crude approximation to this geometry is the use of thin magnetic disks whose diameter is a significant fraction of the lattice constant. The anisotropic shape of the disk induces a magnetization parallel to the superconducting plane, similar to that of the magnetic bar. This was in fact the geometry used by Martín *et al.* [2].

We gratefully acknowledge useful conversations with A. Hoffmann and I. K. Schuller. This research is supported by the NSF through grant no. DMR9801921, and by the UC-CLC program.

-
- [1] D. Weiss, K. von Klitzing, K. Ploog, and G. Weimann, *Europhys. Lett.* **8**, 179 (1989).
 - [2] J. I. Martín, M. Vélez, J. Nogués, and I. K. Schuller, *Phys. Rev. Lett.* **79**, 1929 (1997).
 - [3] M. J. Van Bael, K. Temst, V. V. Moshchalkov, and Y. Bruynseraede, *Phys. Rev. B* **59**, 14674 (1998).
 - [4] J. I. Martín, M. Vélez, A. Hoffmann, I. K. Schuller, and J. L. Vincent, *Phys. Rev. Lett.* **83**, 1022 (1999).
 - [5] I. F. Lyukyutov and V. Pokrovsky, *Phys. Rev. Lett.* **81**, 2344 (1998).
 - [6] M. Tinkham, *Introduction to Superconductivity*, (McGraw-Hill, New York, 1996).
 - [7] J. Pearl, *Appl. Phys. Lett.* **5**, 65 (1964).
 - [8] Z. G. Li and P. F. Carcia, *J. Appl. Phys.* **71**, 842 (1992).
 - [9] An isolated magnet with vertical magnetic moment cannot create a single vortex-antivortex pair that would be stable with respect to annihilation; this statement however does not apply when the magnet is part of an array.
 - [10] A. B. MacIsaac, K. De’Bell and J. P. Whitehead, *Phys. Rev. Lett.* **77**, 739 (1996).
 - [11] M. J. Van Bael *et al.*, cond-mat/9911033 (preprint).
 - [12] J. M. Kosterlitz, D. R. Nelson and M. E. Fisher, *Phys. Rev. B* **13**, 412 (1976).
 - [13] R. Šášík and T. Hwa, in preparation.